Laser and Particle Beams (2002), *20*, 263–268. Printed in the USA.

DOI: 10.1017/S0263034602202165

A laser experiment for studying radiative shocks in astrophysics

X. FLEURY,[1] S. BOUQUET,[1] C. STEHLÉ,[2] M. KOENIG,[3] D. BATANI,[4] A. BENUZZI-MOUNAIX,[3] J.-P. CHIÈZE,[5] N. GRANDJOUAN,[3] J. GRENIER,[6] T. HALL,[7] E. HENRY,[4] J.-P. LAFON,[2] S. LEYGNAC,[2] V. MALKA,[3] B. MARCHET,[8] H. MERDJI,[5] C. MICHAUT,[2] AND F. THAIS[5]

[1]Département de Physique Théorique et Appliquée, Commissariat à l'Énergie Atomique, BP 12, 91680 Bruyères-le-Châtel, France
[2]Département d'Astrophysique Stellaire et Galactique, Observatoire de Paris, 92195 Meudon, France
[3]Laboratoire pour l'Utilisation des Lasers Intenses (LULI), UMR 7605, CNRS–CEA–Université Paris VI–École Polytechnique, 91128 Palaiseau Cedex, France
[4]Dipartimento di Fisica "G. Occhialini," Università di Milano–Bicocca and INFM, Via Emanueli 15, 20126 Milano, Italy
[5]Commissariat à l'Énergie Atomique, DSM, 91191 Gif-sur-Yvette Cedex, France
[6]Commissariat à l'Énergie Atomique, CESTA, BP 2, 33114 Le Barp, France
[7]University of Essex, Colchester CO4 3SQ, United Kingdom
[8]Département de Conception et de Réalisation des Expériences, Commissariat à l'Énergie Atomique, BP 12, 91680 Bruyères-le-Châtel, France

(RECEIVED 15 November 2001; ACCEPTED 12 May 2002)

Abstract

In this article, we present a laboratory astrophysics experiment on radiative shocks and its interpretation using simple modelization. The experiment is performed with a 100-J laser (pulse duration of about 0.5 ns) which irradiates a 1-mm^3 xenon gas-filled cell. Descriptions of both the experiment and the associated diagnostics are given. The apparition of a radiation precursor in the unshocked material is evidenced from interferometry diagrams. A model including self-similar solutions and numerical ones is derived and fairly good agreements are obtained between the theoretical and the experimental results.

Keywords: Interferometry; Laser astrophysics; Radiative precursor; Self similar solutions

1. INTRODUCTION

Shock waves play a significant role in several astrophysical phenomena. Among those, one can mention the explosions of type II supernovæ (SNeII; Zwicky, 1965; Weaver, 1976; Kumagai, 1989; Arnett, 1996; Bethe, 1997). An explosion of this type happens in a massive star when it has come to the end of its life. At that time, the core of the star shrinks and the outer layers of the star are no longer supported. As a consequence, they start collapsing under the effect of gravity. When the core reaches the nuclear density, the outer layers rebound on it, and a highly energetic shock wave is generated. This shock wave moves outward and propagates in a collisional medium at a very high temperature.

In these conditions, the shocked medium produces radiation which heats and modifies the characteristics of matter far away from the place where it is emitted. The unshocked medium is then affected by these radiations: its thermodynamic properties change, modifying in return the propagation of the shock wave. This coupling between a shock and the medium in which it propagates, through radiation, characterizes the radiative shocks.

A good understanding of these waves is a key point in astrophysics, since an accurate description of several stellar phenomena [in addition to SNeII explosions, we can also mention stellar wind emission (Lucy & Solomon, 1970; Garmany *et al.*, 1981) or circumstellar envelop dynamics of evolved stars (Huguet *et al.*, 1994; Huguet & Lafon, 1997)] relies on their relevant modeling. To improve the present knowledge on these waves, experimental simulations with lasers have appeared, in recent years, as a fruitful method of investigation (Bozier *et al.*, 1986, 2000; Farley *et al.*, 1999; Ditmire *et al.*, 2000; Keilty *et al.*, 2000; Shigemori *et al.*, 2000; Kœnig *et al.*, 2001; Lebedev, 2001). Indeed, high-power laser facilities [like the existing ones at the Laboratoire pour l'Utilisation des Lasers Intenses (LULI) at the École Polytechnique, France, or the Ligne d'Intégration Laser (LIL) at the Centre d'Études Scientifiques et Techniques d'Aquitaine, France, and the Laser MégaJoule (LMJ) in the future] enable us now to drive shocks in which the

Address correspondence and reprint requests to: S. Bouquet, Département de Physique Théorique et Appliquée, Commissariat à l'Énergie Atomique, BP 12, 91680 Bruyéres-le-Châtel, France. E-mail: bouquets@bruyeres.cea.fr.

radiative flux prevails over purely hydrodynamic mechanisms of energy transfer like heat conduction. Moreover, in some cases that we will detail in the next section, not only the radiative flux, but also the radiative energy and the radiative pressure are nonnegligible compared to the corresponding hydrodynamic quantities. When this latter situation occurs, we will say that the propagation regime of the shock wave is fully radiative. Different diagnostic methods enable experimental characterization of shock waves. Thus, experimental simulation of radiative shocks will be of great help to go further in the understanding of these complex phenomena.

The aim of the work presented here is to study radiative shocks thanks to a laser experiment performed at the LULI. We will first present an analytical description of a stationary radiative shock, proposed in Bouquet *et al.* (2000). This work gives a condition on the shock velocity such that a full radiative regime could appear. The design of the experiment is based on this condition, since we want to observe a phenomenon where radiative effects are as important as possible regarding the energy of the laser. The experimental setup is described below and we give experimental results which show the radiative behavior of the observed shock wave. We then propose a semianalytical model which enables us to compute the velocity of the radiative precursor.

2. ANALYTICAL DESCRIPTION OF THE RADIATIVE SHOCK

Let us first recall briefly the study presented in Bouquet *et al.* (2000). We consider a plane stationary shock wave traveling through a perfect gas. The region located in front of the shock transition zone is called the upstream region and the region where the gas is compressed after this zone is the downstream region. Matter and radiation are assumed to be at local thermodynamic equilibrium (LTE); therefore radiative energy and pressure are those of an ideal black body. The Rankine–Hugoniot (RH) relations express the balance of each conservative quantity between the upstream and the downstream regions. If we look at these quantities far enough from the transition zone, we can consider that they are uniform and the RH relations appear as a system of algebraic equations.

For hypersonic shock waves, this system can be solved analytically and one can express the ratio between the radiative pressure and the thermal pressure for the shocked medium, $P_{rad_2} = P_{th_2}$ (the subscript 2 refers to the downstream flow), as a function of the shock velocity, D, and of the physical quantities in the unshocked material. The criterion $P_{rad_2}/P_{th_2} \geq 1$, which characterizes a full radiative regime, yields

$$D \geq D_{rad} = \left(\frac{7^7 k^4}{72a} \frac{n_1}{\mu_1^3} \right)^{1/6}, \quad (1)$$

where k, a, n_1, and μ_1 are, respectively, the Boltzmann constant, the first radiative constant, the particle density, and the particle mass in the upstream region (indexed with the subscript 1). The velocity D_{rad} is a threshold between, on one hand, a regime where only the radiative flux plays a role in the dynamics of the shock and, on the other hand, a full radiative regime. On an experimental point of view, the available shock velocities cannot exceed a given value, which depends on the facility. Thus, to make sure that this latter regime could be reached in our laser experiment, we needed to decrease the value of the velocity D_{rad} as much as possible by choosing conveniently the propagation medium. By looking at (1), one can notice that D_{rad} decreases with respect to the particle mass of the medium and increases with respect to its density. For that reason, the experiment was made on a heavy gas, xenon, at a low pressure fixed at around 0.1 atm. This pressure could not be smaller, since, if the gas had been too rarefied, most of the radiation emitted towards the unshocked medium would have been lost. With these conditions, we have $D_{rad} \simeq 25\ \mathrm{km \cdot s^{-1}}$. This shock velocity can be achieved with the facilities of the LULI.

3. EXPERIMENTAL SETUP

Parallelepipedic transparent quartz cells, whose internal volume is around 1 mm^3 (1 mm in each direction), are filled with xenon at pressures of 0.1 and 0.2 atm. One of their sides is made of a three-layer pusher which consists of polystyrene (2 μm thick), titanium (3 μm), and foam (25 μm). This side is to be attacked orthogonally by the beam of the power laser to generate the shock. The polystyrene layer is irradiated first and is ablated to give birth to the shock. The titanium layer plays the role of a shield against X rays which come from the interaction between the laser and the ablator and which are likely to preheat xenon if they are not stopped. The foam layer is able to move at high velocity when the shock arrives because of its low density. It becomes then a fast pusher for the xenon. To generate a plane shock, the laser pulse is focalized uniformly at the center of the ablator and on a circular spot whose diameter is around 250 μm. The extension of this focal spot was maximized, so that, in the neighborhood of the longitudinal axis of the cell (the longitudinal direction is the direction of propagation of the shock), the shock should behave approximately like a plane perturbation. The radiation emitted from the hot and compressed region transfers energy to the unshocked gas and a hot radiative precursor should appear. A global scheme describing the target and the phenomenon is presented in Figure 1.

The whole experimental setup is shown in Figure 2. The laser pulse which is focused on the target is made of three beams at a wavelength $\lambda = 0.53$ μm for a total energy of about 100 J. These beams are delivered by the LULI's nanosecond Nd-glass laser. The pulse duration at full intensity is roughly equal to 500 ps. Taking into account the size of the

https://doi.org/10.1017/S0263034602202165 Published online by Cambridge University Press

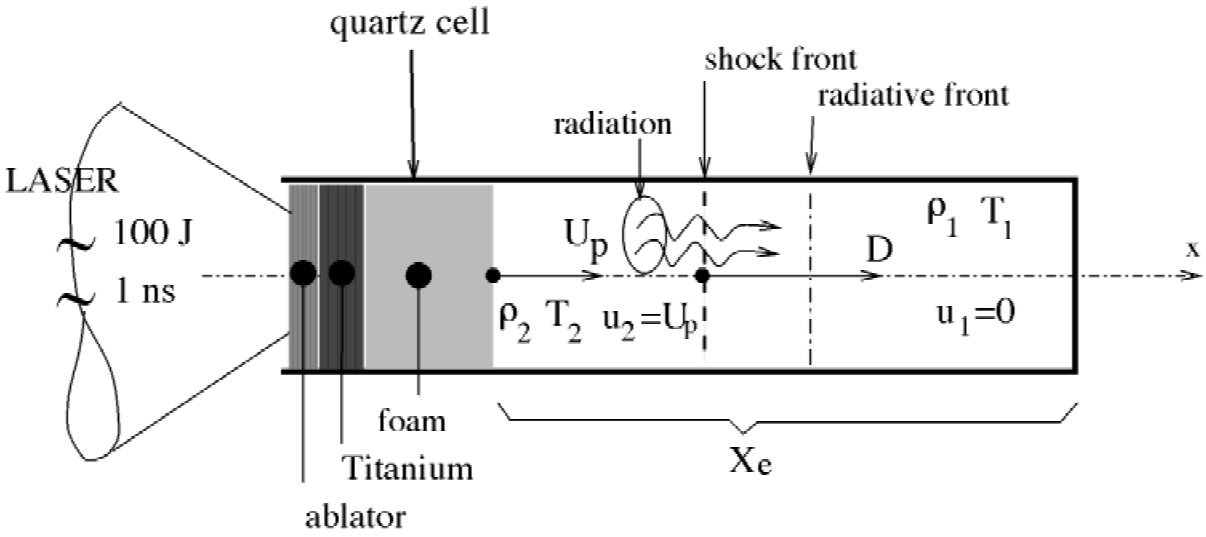

Fig. 1. Target scheme and propagation of the radiative shock. The quantities ρ_α, T_α, u_α ($\alpha = 1, 2$) are, respectively, the mass density, the temperature, and the velocity in the upstream ($\alpha = 1$) or the downstream ($\alpha = 2$) region, while U_p and D denote, respectively, the piston and the shock velocity. The x coordinate refers to the longitudinal position.

focal spot, one can estimate that the energy flux is approximately 5×10^{13} W·cm^{-2}.

Four diagnostics have been settled in. The first one is a self-emission diagnostic. It consists of a streak camera which records the light coming from the rear side of the cell. The second one comprises two streak cameras (VISAR#1 and VISAR#2) with different sensitivities, which enable us to find out the velocity of the foam/xenon interface (VISAR diagnostic). The last ones use a Mach–Zehnder interferometer, which provides an interference picture after the crossing of one of the probe beams through the target. Part of this picture is recorded along a horizontal longitudinal line (longitudinal diagnostic). Another record is done in a transverse direction, at a given longitudinal position (transverse

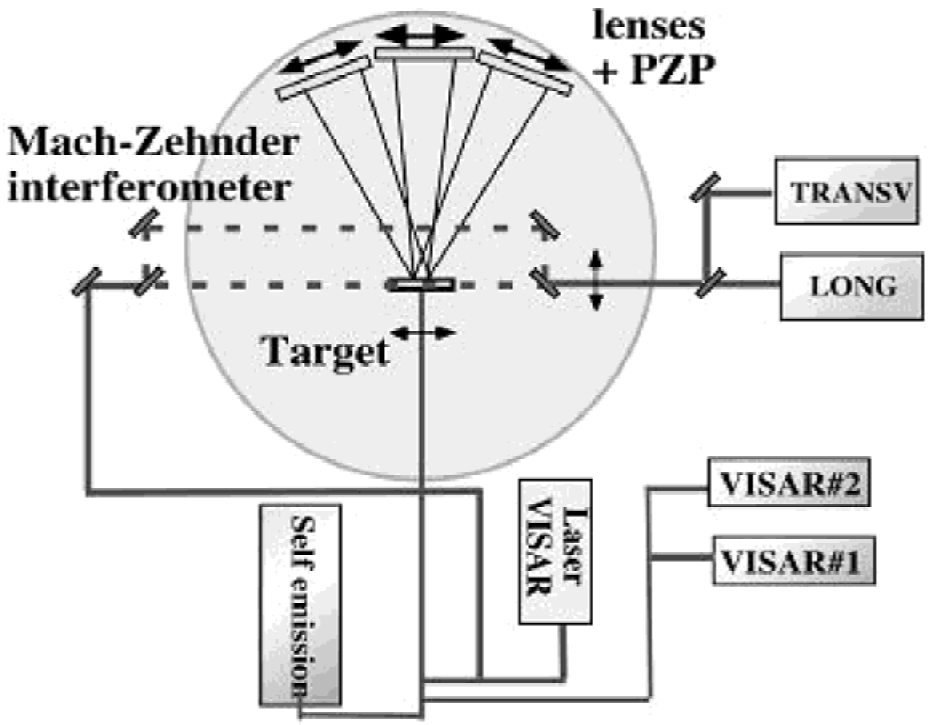

Fig. 2. Experimental setup and diagnostics.

https://doi.org/10.1017/S0263034602202165 Published online by Cambridge University Press

diagnostic). The recording time is about the traveling time of the shock in the cell (about 10 ns). This last two diagnostics, based on interferometry principles (Celliers *et al.*, 1998), should give profiles of the electron density at successive times all along the record.

4. EXPERIMENTAL RESULTS

We will focus here on the results of the most representative laser shot.

For the shot considered, the laser pulse energy was $E_{las} =$ 73 J and the gas pressure 0:2 atm. For these conditions, we have $D_{rad} = 25\ \mathrm{km \cdot s^{-1}}$. The VISAR diagnostic provides $U_p \simeq 60\ \mathrm{km \cdot s^{-1}}$ during the first two nanoseconds of the shock propagation (see Kœnig *et al.*, 2001, for more details).

The most important diagnostic to evidence the radiative behavior of the shock is the longitudinal one, since it accounts for the electron density profile along the shock direction at different times. Indeed, the electron density increases with temperature. Therefore, the detection of a significant electron density beyond the shock front will be the proof that the unshocked medium has been heated. From the measure of the extension of the heated region, one can infer whether this heating is due to a radiative flux or not.

Let us now apply this reasoning to the interferogram displayed in Figure 3. At each time of the record, three regions can be identified within the enlighted zone: a first region where the signal is approximately uniform, a second one where squeezed fringes appear, and a last one where the fringes are parallel and equally spaced. The evolution of the frontiers between these regions has been drawn in Figure 3 with a plain line and a dashed line. These frontiers define two perturbations whose velocities can be measured. We will denote by v_I and v_{II} the velocities corresponding respectively to the dashed and to the plain line. From right to left, after having passed the dashed line, the fringes are getting closer and closer, which is due to an increasing gradient of electron density. Near the plain line, the resolution of the camera cannot separate the fringes any more. This means that high gradients of electron density have been reached and this position must be close to that of the shock discontinuity. The corresponding velocity v_{II} is around $60\ \mathrm{km \cdot s^{-1}}$. It may be attributed to the front shock velocity D. We can conclude that this interferogram shows that a plasma has been created in front of the shock. The extension of this plasma increases with time, since the region between the two lines gets larger. The measurement of the average value of v_I, $\langle v_I \rangle$, gives the expansion speed of the plasma. We get $\langle v_I \rangle \simeq 130\ \mathrm{km \cdot s^{-1}}$, 1.6 ns after the beginning of the record. The extension of this hot zone grows too fast to be a consequence of a heating by conduction only and the region between the two perturbations shows that a radiative precursor is generated.

Moreover, since we have $D \geq U_p \simeq 60\ \mathrm{km \cdot s^{-1}} > D_{rad}$, we conclude that the propagation regime of the shock is fully radiative.

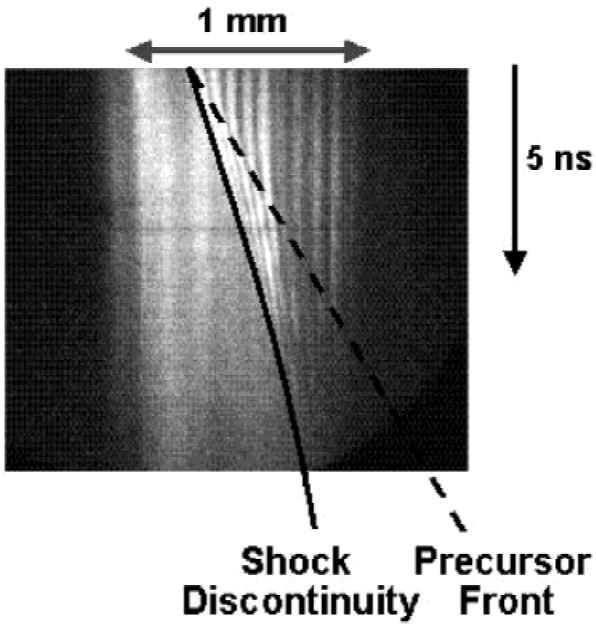

Fig. 3. Interferogram given by the longitudinal diagnostic for a laser shot at the energy $E_{las} = 73$ J on a gas cell at a pressure of 0.2 atm. The side of the cell attacked by the laser is at the left on this picture.

5. ANALYTICAL MODEL OF THE RADIATIVE PRECURSOR

We want now to estimate theoretically the velocity of a radiative precursor in order to interpret the measured value which is twice the shock velocity. For this purpose, we use and extend a model proposed initially by Bozier *et al.* (1986). We report below a semianalytical method of resolution for this approach (Fleury *et al.*, 2001).

The model consists of the energy conservation equation in the precursor, where the gas is at rest. We write this equation as

$$\frac{\partial e}{\partial t} = -\frac{\partial q_{rad}}{\partial x}, \tag{2}$$

where $e = c_v \rho T$ is the density of thermal energy (ρ and T are the mass density and the temperature of the gas, respectively, and c_v is the specific heat) and where q_{rad} is the radiative flux. The coordinate x refers to the longitudinal position and t is the time. We have, in the diffusion approximation, $q_{rad} = -[\lambda(\rho, T)c/3][\partial(aT^4)/\partial x]$, where λ is the photon mean free path and c is the speed of light. As for the data characterizing the gas, that is, c_v and $\lambda(\rho, T)$, we take the values given in Bozier *et al.* (1986). We have then $c_v =$ $1850\ \mathrm{J \cdot K^{-1} \cdot kg^{-1}}$ and $\lambda(\rho, T) = \theta T^n/\rho^m$ where $n = 2.2$, $m = 1.2$, and $\theta = 9.16 \times 10^{-16}$ MKSA. The precursor

https://doi.org/10.1017/S0263034602202165 Published online by Cambridge University Press

receives from the shock the following radiative flux $q_* = \rho_1 D U_p^2/2$. We may write the following boundary condition

$$q_{rad}(x=0) = q_*, \tag{3}$$

where $x = 0$ is the position of the interface foam/xenon before the shock arrives. According to the derivation of the model, this condition should be imposed on the shock front, that is, at $x = D \times t$. Nevertheless, we have checked that the value $q_{rad}(Dt)$ numerically computed out of Eqs. (2) and (3) is still close to the value q_*. Setting the boundary condition at a fixed point simplifies greatly the resolution of the problem.

Equations (2) and (3) form a nonlinear heat equation problem whose unknown is the temperature in the precursor. This problem can be solved numerically, once an initial condition is given. It can also be solved by looking for particular solutions. Indeed, we can prove that it is invariant under the action of a rescaling group. It must then admit self-similar solutions (SSS). Those SSS will verify a second-order ordinary differential equation (ODE) that we do not write here (Fleury *et al.*, 2001). This equation can be solved numerically as well. Both solutions to the problem (2, 3) and to the corresponding ODE problem are represented in Figure 4.

The correspondence between the two solutions is quite good and it seems that the SSS are attractors for the partial differential equation problem (2, 3). Thus, we may use the SSS to compute the physical quantities of interest. For the averaged velocity of the precursor front in the time interval $[0, \tau]$, we obtain

$$\langle v_{rf}\rangle(\tau) = 1.2 \times \left(\frac{1}{2c_v}\right)^{(n+4)/(n+5)} \left(\frac{8\theta ac}{3(n+4)}\right)^{1/(n+5)} \times (DU_p^2)^{(n+3)/(n+5)} \left(\frac{1}{\rho_1}\right)^{(m+1)/(n+5)} \left(\frac{1}{\tau}\right)^{1/(n+5)}. \tag{4}$$

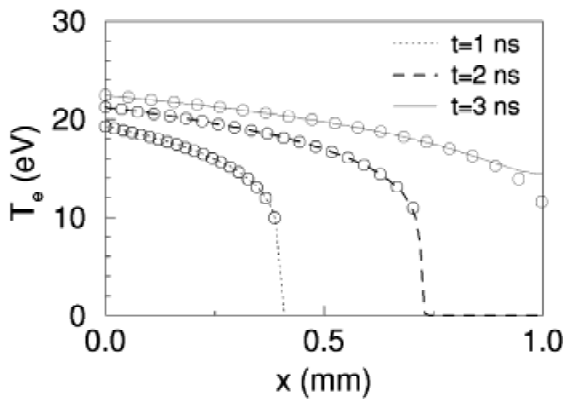

Fig. 4. Temperature in the precursor at different times. The position $x = 0$ refers to the position of the interface foam/xenon before the arrival of the shock. Lines are the profiles obtained by solving problem (2,3); circles give the profiles of the SSS.

To apply this formula to the case presented in the previous section, we use $D \simeq U_p \simeq 60\ \mathrm{km \cdot s^{-1}}$. Computing the average precursor velocity at the time $\tau = 1.6$ ns at which it has been measured, we get $\langle v_{rf}\rangle = 315\ \mathrm{km \cdot s^{-1}}$. Similar computations can be done for laser shots with different conditions. They are compared with measurements in Table 1.

The computed precursor velocity $\langle v_{rf}\rangle$ is much higher than $\langle v_{II}\rangle$, interpreted as the shock speed, in the three cases. This reproduces the fact that the precursor propagates much faster than the shock, as observed in the experiment.

The model gives velocities which are of the same order of magnitude as the measured values, but they are overestimated. This gap between the model and the reality is probably due to the assumption made on the radiative flux. Indeed, the diffusion approximation was made to provide this flux and yet this approximation is valid only when the mean free path of photons is small with respect to the variation scale of radiative energy. Here we have $T \sim 20$ eV (see Fig. 4) and, consequently, $\lambda \sim 0.5$ mm. According to Figure 4, we are at the frontier of this condition. A more detailed treatment of radiation would probably improve these results. Though the overestimation of the precursor velocity, the values obtained for temperature ($T \sim 20$ eV) are very close to what is computed by other approaches, using hydrodynamic codes (Kœnig *et al.*, 2001, Fleury *et al.*, 2001).

6. CONCLUSION

In this article, we have presented some of the results (both theoretical and experimental) of a study of radiative shocks. The radiative precursor characterizing such a shock wave has been actually observed and it was done for the first time in full radiative regime. We proposed a first approach to model the propagation of the radiative precursor in which an analytical formula of the velocity of the radiative front has been derived. The validity of this formula was evidenced numerically. Thanks to this approach, we obtained the order of magnitude of the precursor velocity and a good estimation of its temperature.

Further studies should focus on the modelization of radiative transfer out of LTE. Moreover, a second campaign of

Table 1. *Comparison between the measured precursor velocities $\langle v_I\rangle$ and the estimated precursor velocities $\langle v_{rf}\rangle$ for different shots.*[a]

P (atm)	E_{las} (J)	$\langle v_{II}\rangle$ ($\mathrm{km \cdot s^{-1}}$)	$\langle v_I\rangle$ ($\mathrm{km \cdot s^{-1}}$)	τ (ns)	$\langle v_{rf}\rangle$ ($\mathrm{km \cdot s^{-1}}$)
0.2	73	60	130	1.6	315
0.1	57	48	75	5	205
0.1	80	58	100	4	318

[a]Each laser shot is characterized by its energy E_{las} and the pressure P of the xenon in the target. The velocities $\langle v_I\rangle$ and $\langle v_{II}\rangle$ are average velocities measured on a time interval $[0, \tau]$. The error on these measurements is less than 10%. The estimated velocity $\langle v_{rf}\rangle$ is an average over the same interval. To compute it, we used the value of $\langle v_{II}\rangle$ as the piston velocity.

https://doi.org/10.1017/S0263034602202165 Published online by Cambridge University Press

experiments planned for the beginning of 2002 will be the opportunity for looking deeper into the effects of the full radiative regime and into the influence of the experimental conditions.

ACKNOWLEDGMENTS

The authors thank Françoise Gex and Patrice Barroso (Observatoire de Paris/PHT), Loïc Polès (CEA/VALDUC), and Benoît Cathala (CEA/CESTA) for manufacturing the targets, and Philippe Moreau (LULI) for his contribution to the experiment. This work was supported by the Programme National de Physique Stellaire, the Observatoire de Paris, and the Groupe d'Investigation des Applications Scientifiques du LMJ.

REFERENCES

Arnett, D. (1996). *Supernovæ and Nucleosynthesis*, Princeton, NJ: Princeton University Press.
Bethe, H.A. (1997). *Astrophys. J.* **490**, 765–771.
Bouquet, S., Teyssier R. & Chièze J.-P. (2000). *Astrophys. J. Supp.* **127**, 245–252.
Bozier, J.-C. *et al.* (1986). *Phys. Rev. Lett.* **57**, 1304–1307.
Bozier, J.-C. *et al.* (2000). *Astroph. J. Supp.* **127**, 253–260.
Celliers, P.M. *et al.* (1998). *Applied Phys. Lett.* **73**, 1320–1323.
Ditmire, T. *et al.* (2000). *Astrophys. J. Supp.* **127**, 299–304.
Farley, D.R. *et al.* (1999). *Phys. Rev. Lett.* **83**, 1982–1985.
Fleury, X. *et al.* (2002). The radiative shock: Theory, laser experiments and interpretation. *Proc. 2nd Conf. Inertial Fusion Sciences and Applications*. Kyoto, in press.
Garmany, C.D. *et al.* (1981). *Astrophys. J.* **250**, 660–676.
Huguet, E. *et al.* (1994). *Astron. Astrophys.* **290**, 518–530.
Huguet, E. & Lafon, J.-P.J. (1997). *Astron. Astrophys.* **324**, 1046–1058.
Keilty, K.A. *et al.* (2000). *Astrophys. J. Supp.* **538**, 645–652.
Kœnig, M. *et al.* (2002). Radiative shock experiment using high power laser. *Proc. Conf. Shock Compression of Condensed Matter, 12th APS meeting*. Atlanta, in press.
Kumagai, S. *et al.* (1989). *Astrophys. J.* **345**, 412–422.
Lebedev, S.V. (2001), astro-ph/0108067.
Lucy, L.B. & Solomon, P.M. (1970). *Astrophys. J.* **159**, 879–893.
Shigemori, K. *et al.* (2000). *Astrophys. J. Lett.* **533**, L159–L162.
Weaver, T.A. (1976). *Astrophys. J. Supp.* **32**, 233–282.
Zwicky, F. (1965). In *Stellar Structure* (Allen, L.H. & MacLaughlin, D.B., Eds.). Chicago: Chicago University Press.